ANALYSIS OF LONGITUDINAL ACCELERATOR INSTABILITIES

Robert L. Pease*
Princeton-Pennsylvania Accelerator
Princeton, New Jersey**

Summary. A sufficient stability condition for uniform coasting beams in cyclic particle accelerators is derived from Neil and Sessler's dispersion equation. Specific conditions are worked out for various injection patterns. The instability threshold depends fairly strongly upon the particle density distribution across the tank, and upon whether operation is below or above transition energy. For the latter case, the optimum distribution (allowing the largest number of particles in the beam) is derived. The possibility is investigated, using Nyquist diagrams, of injecting more particles by operating in a superstable state - one which depends for its stability on the low resistance of the tank walls. It is shown that any practical improvement by this means is probably illusory.

Introduction

Older theories[1,2] of longitudinal accelerator instabilities, which were based on an analysis of the negative mass instability, were inadequate in that (1) they did not predict instabilities below transition energy[3] and (2) they predicted an energy spread needed to suppress instabilities above transition which was too low.[4] A more comprehensive theory, which included resistive effects, was developed by Neil and Sessler.[5] The aim of this paper is to work out some of the consequences of Neil and Sessler's theory.

The Theory of Neil and Sessler

Neil and Sessler[5] showed that collective longitudinal oscillations in a uniform coasting beam in a cyclic particle accelerator could be described by the plasma dispersion equation

$$U' + iV' = n k_o \delta^2 \left(\frac{U + iV}{U^2 + V^2} \right) = \int_{-1}^{1} \frac{dF}{d\xi} \frac{d\xi}{\xi - \xi_1} \quad . \tag{1}$$

The quantities U and V are accelerator parameters given by[5]

$$U \equiv (N e^2 n/R)(1 - \beta^2) X \left[1 + 2 \ln (b/a) \right] \quad \text{(coax, esu)} \tag{2a}$$

$$V \equiv (N e^2/b)(2\beta) \sqrt{\omega\mu/8\pi\sigma} \tag{2b}$$

for a coaxial geometry, in esu; for a rectangular geometry† more complicated expressions are given in Reference 5. N is the number of particles in the beam, a is the beam radius, b is the tank radius, R is the average path radius, $\beta \equiv v/c$, n is the harmonic number of the instability relative to the average circulation frequency, ω is the instability angular frequency, and μ and σ are constitutive parameters of the vacuum chamber walls. Experimentally

$$V \ll U. \tag{2c}$$

The running parameter $\xi \equiv w/\delta$, where w is a canonical variable defined in terms of energy E and particle circulation frequency f_c

$$w \equiv \int_{\text{center}} \frac{dE}{f_c(E)} \simeq 2\pi \left\{ \begin{array}{l} \text{actual angular momentum -} \\ \text{angular momentum at center of beam} \end{array} \right. \tag{3}$$

and δ is the half-width of w across the tank; hence $-1 \le \xi \le 1$. The quantity w_1 is related to the difference between the instability angular frequency ω and the average particle circulation angular frequency ω_o through

$$\omega = n \omega_o + n k_o w_1 \tag{4}$$

where k_o is defined through

$$k_o \equiv 2\pi f_c \frac{df_c}{dE} \quad . \tag{5}$$

The function $F(\xi)$ describes the density of particles as a function of ξ, and hence essentially as a function of position across the vacuum chamber.

Note that Equation (1) differs from the formally similar simple plasma equation[6] in that the velocity distribution is narrow and finite, and in that it is possible that $V' \neq 0$ (resistive instability) and/or $U' < 0$ (negative mass instability). Some of the normal plasma "rules" no longer apply, e.g., an $F(\xi)$ with a single maximum no longer guarantees stability.

From (1) and (2c) we can write

$$\delta \simeq \sqrt{U'} \sqrt{U/nk_o} \quad . \tag{6}$$

*On leave from Brooklyn College of the City University of New York, Brooklyn 10, N. Y.

**Work supported by the AEC.

†A quite accurate U can be obtained for a strip beam if 2 ln (b/a) is replaced by $Z_o/30$, where Z_o is the characteristic impedance in ohms between beam and tank considered as a transmission line.

Neil and Sessler,[5] in addition to deriving (1), discussed stabilization with resonance-line and Gaussian $F(\xi)$, derived the necessary stability condition for any $F(\xi)$ of finite range that*

$$|U'| > 1, \text{ or } \delta > \sqrt{U/n|k_o|} \text{ (necessary)} \qquad (7)$$

and stated that Equation (7) is not too far from a sufficient stability condition if σ is sufficiently large.

This paper reports work on sufficient stability conditions, optimum stable distributions and superstable states.

Sufficient Stability Conditions

From the dispersion equation (1) we can see that U' and V' are analytic functions of $\xi_1 = \alpha + i\beta$ except along the path $-1 \leq \alpha \leq 1$, $\beta = 0$, and hence obey Laplace's equation in the ξ_1 plane except along this path. Thus any maximum or minimum of U' will lie on the curve

$$U'(\alpha) \equiv U'(\alpha,0) = P\int_{-1}^{1} \frac{dF}{d\xi}\frac{d\xi}{\xi-\alpha}. \qquad (8)$$

(The U' surface may be visualized as a membrane held by a wire of shape (8) and clamped at zero displacement at infinity.) The system will be certainly stable if no collective solution exists; this will be so if the experimental value of U' lies completely above the U' surface (for $k_o > 0$) or completely below it (for $k_o < 0$). Since the extrema are contained in curve (8), a strong sufficient condition for stability is

$$U' > \max\left[U'(\alpha)\right], \quad k_o > 0 \qquad (9a)$$

$$U' < \min\left[U'(\alpha)\right], \quad k_o < 0 \ . \qquad (9b)$$

As examples consider the two injection patterns

$$F_1(\xi) \equiv (3/4)(1-\xi^2) \qquad (10a)$$

$$F_2(\xi) \equiv (15/16)(1-\xi^2)^2 \qquad (10b)$$

which are plotted in Figure 1 and have the respective stability curves

$$U_1'(\alpha) = -3 + \frac{3\alpha}{2}\ln\left|\frac{1+\alpha}{1-\alpha}\right| \qquad (11a)$$

and

$$U_2'(\alpha) = -5 + \frac{15}{2}\alpha^2 + \frac{15}{4}\alpha(1-\alpha^2)\ln\left|\frac{1+\alpha}{1-\alpha}\right|. \qquad (11b)$$

which are shown in Figure 2.

For operation above transition ($k_o < 0$), the system is stable when the experimental U' lies below the lowest point on the $U'(\alpha)$ curve, or, for distributions $F_1(\xi)$ and $F_2(\xi)$ respectively,

$$U_1' < -3, \text{ or } \delta_1 > \sqrt{3}\sqrt{U/n|k_o|} \text{ (sufficient)} \quad (k_o < 0). \qquad (12a)$$

$$U_2' < -5, \text{ or } \delta_2 > \sqrt{5}\sqrt{U/n|k_o|} \text{ (sufficient)} \quad (k_o < 0) \qquad (12b)$$

On the other hand, below transition, the condition is

$$U_1' > \infty \quad \text{(logarithmically unstable)} \qquad (13a)$$

$$U_2' > 3.1, \text{ or } \delta_2 > \sqrt{3.1}\sqrt{U/nk_o} \text{ (sufficient)} \quad (k_o > 0) \qquad (13b)$$

Hence the parabolic distribution, which will permit the use of 23 % smaller energy spread or the injection of 67 % more particles above transition, is almost useless below transition. (It is not, however, true that above transition the fatter the pattern the better, for the logical extension of F_1 - a rectangular pattern - turns out to be unstable both above and below transition).

As a first approximation, we could use F_1 above transition and F_2 below; however, we can do much better above transition and a little better below.

Optimum Distributions

One way to do better is to cut and try, as follows; consider the case $k_o < 0$ (above transition) for concreteness: Start with, say, $F_1(\xi)$, and draw $U_1'(\alpha)$. Then choose some other distribution, for example $F_f(\xi) \equiv (5/8)(1-\xi^4)$, compute its stability curve $U_f'(\xi)$, and plot it on the same graph as $U_1'(\alpha)$. (See Figure 3). Note that the curves $U_1'(\alpha)$ and $U_f'(\alpha)$ intersect at the point $\alpha = 0.43$, $U'(\alpha) = -2.40$. Measure the respective slopes m_1 and m_f at this point. Then a composite curve

$$U_{1f}' = \frac{|m_f|U_1' + |m_1|U_f'}{|m_1| + |m_f|} \qquad (14)$$

will have automatically a zero slope at the point of intersection. If we are fortunate - and we are in this example - this point will be the minimum. Hence if we use not $F_1(\xi)$ but the distribution

$$F_{1f} = \frac{|m_f|F_1 + |m_1|F_f}{|m_1| + |m_f|} \qquad (15)$$

*As a numerical example, Eqn. (6) may be rewritten in terms of energy for the Princeton-Pennsylvania Accelerator at injection as $\Delta E \simeq \sqrt{U'}\sqrt{N/10^{12}}$ (27 keV), where E is the total energy spread. The maximum permitted energy spread across the tank at injection is about 41 keV. Hence from Eqn. (7) there will certainly be instability at injection with about 2.3×10^{12} particles in an ideal uniform 360° beam.

we will have raised the minimum from -3 to -2.40, i.e., permitted the injection of 25% more particles.

Suppose we were able to continue improving the curve this way, getting a flatter and flatter bottom. The best possible $U'(\alpha)$ would be one with a flat bottom from $\alpha = 0$ to $\alpha = 1$; we could do no better, for if F were changed by adding a little at one value of ξ, we would have to subtract a little at another value of ξ; but then the flat curve would have a downward and an upward bump, and the minimum would be lower. The optimum $F(\xi)$ above transition is simply the normalized integral of the inverse finite range Hilbert transform[7] of a constant, and is

$$F^{opt}_{k_o<0}(\xi) = F_{1/2}(\xi) \equiv (2/\pi)\sqrt{1-\xi^2}\ ; \tag{16}$$

the requirement of normalization gives us the stability condition

$U' < -2$, or

$$\delta_{1/2} > \sqrt{2}\sqrt{U/n|k_o|} \quad \begin{matrix}(\text{sufficient})\\(k_o<0)\end{matrix} \tag{17}$$

The optimum $F(\xi)$ above transition is shown in Figure 4, and its stability curve is shown in Figure 5. A distribution curve $F(\xi)$ which is either blunter or sharper than $F_{1/2}(\xi)$ will require a larger $|U'|$ for stability.*

Below transition, I have not been able to find an optimum, but quite a large number of curves give about the same maximum so I doubt if the optimum would give a striking improvement. A good curve is

$$\begin{aligned} F^{good}_{k_o>0} &= 0.293\, F_{3/2}(\xi) + 0.707\, F_{5/2}(\xi) \\ &= 0.293\,(8/3\pi)(1-\xi^2)^{3/2} \\ &\quad + 0.707\,(16/5\pi)(1-\xi^2)^{5/2} \end{aligned} \tag{18}$$

which resembles F_2 but leads to the slightly better stability condition

$$U' > 2.83, \text{ or } \delta > \sqrt{2.83}\sqrt{U/nk_o} \quad \begin{matrix}(\text{sufficient})\\(k_o>0)\end{matrix} \tag{19}$$

*To return to our numerical example, the optimum distribution (16) would permit the P.P.A. at injection to carry about 1.2×10^{12} particles (uniformly distributed in azimuth). For the parabolic distribution F_- of Eqn. (10a) the number would be about 8×10^{11}; for a sensible distribution chosen or required on other grounds the number of particles might go as low as 5×10^{11}.

Superstability

The sufficient stability conditions derived so far have been independent of V', i.e., independent of the wall parameters. They are, in theory, unnecessarily severe. For the most liberal stability condition one may draw a Nyquist diagram.[6] This is a plot of V' vs. U' as ξ_1 travels around the circumference of the unstable region; the system is stable if and only if the operating point (actual U', V') lies outside the diagram. In our case

$$V'(\alpha,0\pm) = \pm\,\pi\,(dF/d\xi)_{\xi=\alpha}\ . \tag{20}$$

The Nyquist diagram for F_2 is shown in Figure 6. Points in the shaded region ($U' < -5$ or $U' > 3.1$) satisfy our stability condition. The cross-hatched region, in which the system is stable for V' small enough (σ large enough), may be called the superstable region. By operating in this region, it would appear possible, for small V', to use the less stringent stability condition $U' > 2.5$ and operate with 24% more particles in the accelerator.

But we need not stop there. If we used a sufficiently sharp distribution - almost a delta function - we could bring the mouth of the indentation all the way to +1. Thus for sufficiently small V' it would appear possible to use the necessary condition (7) as a sufficient condition, as was stated in Reference 5, and cram 3.1 times as many particles into the accelerator as would be permitted by (13b). We could also indent to the left as far as -1 by using a sufficiently blunt distribution - almost a rectangle.

Unfortunately, in practice any hope of superstable operation is probably illusory because of the impossible demands made on the flatness of $F(\xi)$. For suppose there were a very small ripple in $F(\xi)$, of amplitude 0.001 and wavelength 0.001, i.e.,

$$\Delta F(\xi) = 0.001 \sin \frac{2\pi}{0.001}\xi\ . \tag{21}$$

Then V' would fluctuate up and down with an amplitude of about 20; the real Nyquist diagram would not look like Figure 6 at all, but would have violent up and down fluctuations, and every point in the cross-hatched area would at some time be inside the diagram. Hence operation in the superstable region would actually be unstable, and conditions (9) would, in fact, be the most lenient possible.

Acknowledgements

I am indebted to Drs. M. Q. Barton, M. G. White, F. C. Shoemaker and J. W. Benoit, and also to members of the Princeton Plasma Physics Laboratory, for helpful discussions, to Mr. Francis Allotey for a summer's help with the analytical and computational work, and in particular to Dr. A. M. Sessler for extensive correspondence.

References

1. A. A. Kolomensky and A. N. Lebedev, Proc. Intl. Conf. on High En. Accel. & Instr., Geneva, 1959, 115-124 (1959)

2. C. E. Nielsen, A. M. Sessler & K. R. Symon, Proc. Intl. Conf. on High En. Accel. & Instr., Geneva, 1959, 239-252 (1959)

3. C. D. Curtis et al., Proc. Intl. Conf. on High En. Accel., Dubna, 1963, 620-652 (1964)

4. M. Q. Barton, Proc. Intl. Conf. on High En. Accel., Dubna, 1963, 157-160 (1964)

5. V. K. Neil and A. M. Sessler, Lawrence Rad. Lab. Report UCRL-11089 (23 October 1963, revised 29 September 1964), to be published in Rev. Sci. Instr.

6. See for instance J. D. Jackson, J. Nucl. Energy C1, 171-89 (1960)

7. H. Sohngen, Math. Zeits. 45, 245-64 (1939)

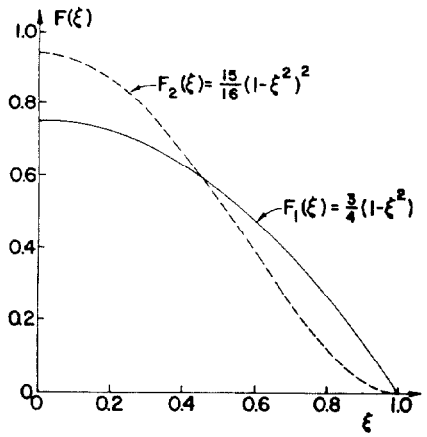

Fig. 1. Parabolic (F_1) and quartic (F_2) particle density distributions across the vacuum chamber. Half of curve ($\xi \geq 0$) shown.

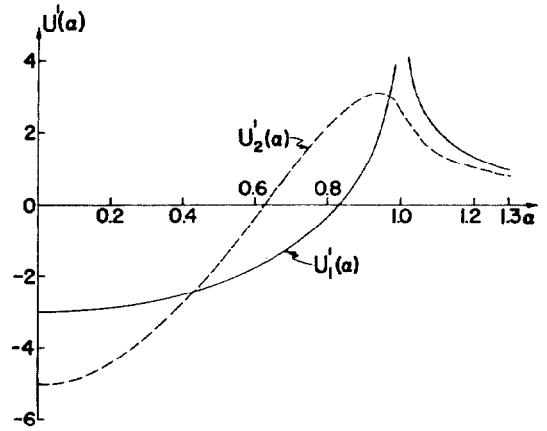

Fig. 2. Stability curves for parabolic (U_1') and quartic (U_2') distributions. Half of curve ($\alpha \geq 0$) shown.

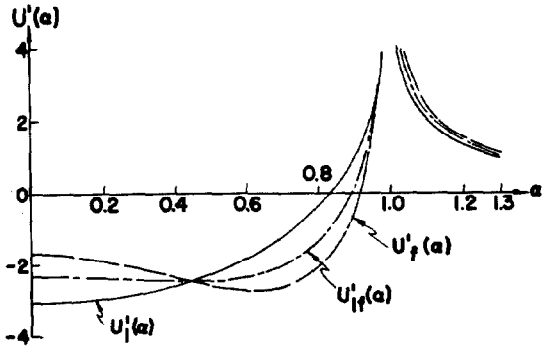

Fig. 3. An optimized composite stability curve (U'_{lf}) - a linear combination of U'_l and U'_f chosen to have zero slope at their intersection. Half of curve ($\alpha \geq 0$) shown.

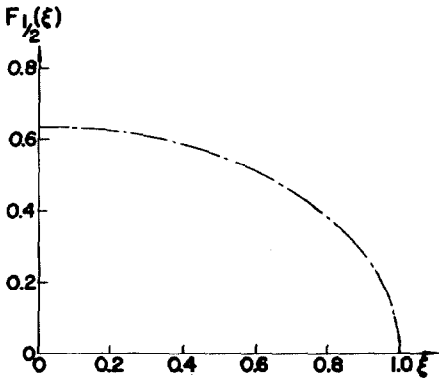

Fig. 4. Optimum distribution curve for operation above transition. Half of curve ($\xi \geq 0$) shown).

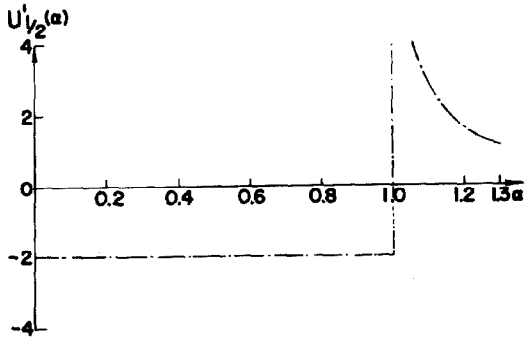

Fig. 5. Stability curve for optimum distribution above transition. Half of curve ($\alpha \geq 0$) shown.

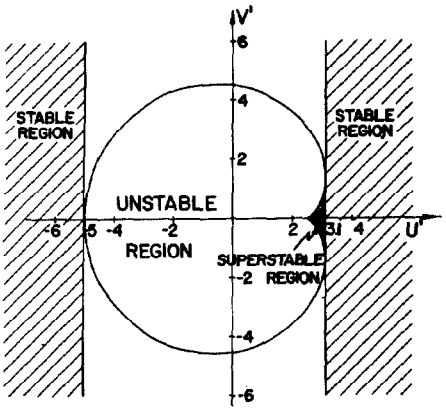

Fig. 6. Nyquist diagram for F_2.